

Local analysis of the history dependence in tetrahedra packings

N. Nirmal Thyagu,^{1,2} Max Neudecker,¹ Simon Weis,³ Fabian M. Schaller,^{3,4} and Matthias Schröter^{1,5,*}

¹Max Planck Institute for Dynamics and Self-Organization (MPIDS), 37077 Goettingen, Germany

²Division of Physics, School of Advanced Sciences, VIT Chennai, Chennai - 600127, India

³Institut für Theoretische Physik I, Friedrich-Alexander-Universität, 91058 Erlangen, Germany

⁴Institute of Stochastics, Karlsruhe Institute of Technology, 76049 Karlsruhe, Germany

⁵Institute for Multiscale Simulation, Friedrich-Alexander-Universität, 91052 Erlangen, Germany

(Dated: October 22, 2018)

The mechanical properties of a granular sample depend frequently on the way the packing was prepared. However, it is not well understood which properties of the packing store this information. Here we present an X-ray tomography study of three pairs of tetrahedra packings prepared with three different tapping protocols. The packings in each pair differ in the number of mechanical constraints C imposed on the particles by their contacts, while their bulk volume fraction ϕ_{global} is approximately the same. We decompose C into the contributions of the three different contact types possible between tetrahedra – face-to-face (F2F), edge-to-face (E2F), and point contacts – which each fix a different amount of constraints. We then perform a local analysis of the contact distribution by grouping the particles together according to their individual volume fraction ϕ_{local} computed from a Voronoi tessellation. We find that in samples which have been tapped sufficiently long the number of F2F contacts becomes an universal function of ϕ_{local} . In contrast the number of E2F and point contacts varies with the applied tapping protocol. Moreover, we find that the anisotropy of the shape of the Voronoi cells depends on the tapping protocol. This behavior differs from spheres and ellipsoids and poses a significant constraint for any mean-field approach to tetrahedra packings.

I. HISTORY DEPENDENCE IN GRANULAR MATTER

A number of experiments have shown that the mechanical properties of apparently identical granular samples will differ depending on how they were prepared. Examples include the volume response to shear [1], the force moment tensor in tapped packings [2–4], the increase of pressure with depth in a granular column [5–8], or the pressure distribution [9] below a sandpile. Another type of history dependent behavior, which is sometimes referred to as memory effect, can be seen if a sample is compactified, e.g. by shearing or tapping with a driving strength s_i , to a specific volume fraction ϕ_{global}^0 . If the driving strength is then changed to some new value s_0 , it is found that the subsequent evolution of ϕ_{global} differs for different values of s_i [10, 11]; even though all samples now start at ϕ_{global}^0 and are driven with the same strength s_0 . A similar effect was found in granular gases [12].

In some sense the term history dependence simply expresses the fact that ϕ_{global} alone does not provide a complete description of the state of the packing. Given that the mechanical properties of the sample originate from forces transmitted between particles at their contacts it seems natural to extend the description by including information on a) the number and spatial structure of the contacts, and b) the distribution of contact forces. Moreover we might want to include, for reasons shown below, c) properties of the Set Voronoi cells surrounding each

particle. (The Set Voronoi cell of a given particle comprises all points which are closer to the surface of the particle than to the surface of any other particle [13–15].)

Option a) has interesting theoretical consequences. This paper studies pairs of hard, frictional tetrahedra packings which have approximately the same ϕ_{global} but differ in their contact numbers Z . Such behavior is clearly beyond the reach of the Jamming paradigm which has been developed for soft, frictionless spheres [16, 17] and where Z is considered to be a function of ϕ_{global} alone.

The reason for this failure is not even primarily the shape of the particles: In the Jamming paradigm both ϕ_{global} and Z are controlled simultaneously by the compression of the soft particles. In contrast, granular particles change their contact number by changing their local geometry, not by compression. For tapped spheres and ellipsoids [18], Z is controlled by the local volume fraction ϕ_{local} which is computed for each individual particles by dividing its volume by the volume of its Voronoi cell [19]. This behavior is in good agreement with statistical mechanics approach [20–22], where Z is computed from a mean-field approximation of ϕ_{local} .

Recently there has been some effort to evolve the Jamming paradigm into a theory which describes history dependence [23, 24]; if this approach can be expanded to describe also frictional and hard particles it would be very valuable.

Option b) is directly connected to the fact that frictional packings at finite pressures are hyperstatic [25–29] i.e. there exist many possible force configurations which fulfill a set of given boundary conditions [30]. Measuring the distribution of contact forces experimentally is a hard problem; it has presently only been achieved in

* matthias.schroeter@ds.mpg.de

systems of compressive particles [31, 32] or photoelastic discs [33]. Experiments with the latter method find a clear dependence on the preparation protocol [34].

Option c) might initially not look too promising: at least for spheres neither the distribution of the volumes of the Voronoi cells [35] nor the distribution of their shapes [36] shows any signature of the preparation conditions. However, for packings of tetrahedra we find that the preparation history does indeed influence the shape and size distribution of the Voronoi volumes.

II. PACKINGS OF TETRAHEDRA

An interesting difference between spheres and tetrahedra is that the latter have not only one but four different types of contacts: face-to-face (F2F) contacts, which are mechanically equivalent to 3 individual point contacts, edge-to-face (E2F) contacts (equivalent to two point contacts) and the vertex-to-face (V2F) and edge-to-edge (E2E) contacts which we group here as point contact.

This distinction is important because the different contact types fix each a different number of degrees of freedom. The total number of constraints of a particle C is therefore $\sum_i C_i$ where i goes over the three contact types (F2F, E2F, point). Each C_i equals $m_i Z_i$ where Z_i is the respective contact number and m_i the number of constraints per particle fixed by this type of contact. The different values of m_i can be understood for frictional contacts as follows: All contacts impose 3 translational constraints, E2F contacts add 2 rotational constraints (thus, a total of 5 constraints), F2F contacts prohibit 3 different rotations (thus, a total of 6 constraints). As these constraints are shared between two tetrahedra, we obtain the constraint multipliers $m_{F2F} = 3.0$, $m_{E2F} = 2.5$, and $m_{V2F} = m_{E2E} = 1.5$.

Each tetrahedron has 6 degrees of freedom (3 translations and 3 rotations), therefore a mechanical stable packing requires C to be at least 6, the so-called isostatic contact number. However, typical packings of frictional tetrahedra have C values in the range 12 to 18 [37] and are therefore strongly hyperstatic [38]. Contrary claims of isostaticity [39] are based on the erroneous use of frictionless constraint multipliers m_i while analyzing experimental i.e. frictional packings. (Due to the absence of tangential forces the frictionless m_i are always smaller than their frictional counterparts.)

Because of the importance of the constraint number for the mechanical properties, we will discuss in the remainder of this paper C rather than Z .

Packings of frictionless tetrahedra have recently been an active field of research because of the existence of quasi-crystals [40], hyperuniformity [41], the effect of altered particle shape on packing density [42–45], the distribution of contact types [46–48], and the behavior of binary systems of tetrahedra and octahedra [49]. Theoretical approaches include a mean field ansatz [21, 22] and a local motif analysis [50–52]. Moreover there has

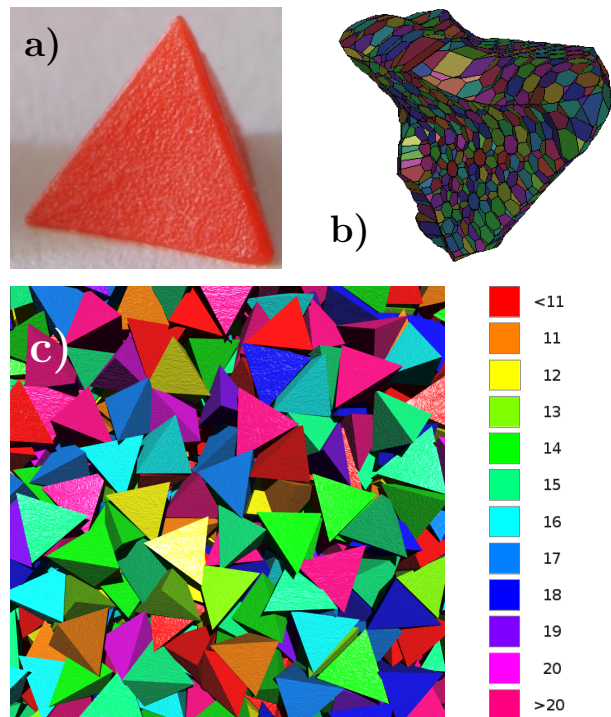


FIG. 1. Tetrahedra packing. **a)** Polypropylene particle made by injection moulding, the edge length is 7mm. **b)** Set Voronoi cell around a tetrahedron with a local volume fraction of 0.52. The Set Voronoi tessellation is computed by spawning 514 point on the surface of each tetrahedron and them merging the Voronoi cells of these points. **c)** Rendering of an interior section of a tetrahedra packing after all particles have been identified from an X-ray tomogram. Particles are colored according to the number of constraints fixed by their neighbors. The global volume fraction is 0.53, the average constraint number is 15.5.

been a quest for the densest tetrahedra packing [53–55], which is presently believed to be at $\phi_{\text{global}} \approx 0.8563$ [56].

Experiments using necessarily frictional tetrahedra explore a much lower range of ϕ_{global} [57] than the numerical studies of frictionless tetrahedra described above. They have been characterized with respect to their mechanical properties under uniaxial compression [58, 59] and shown to have history dependent values of C and Z for identical values of ϕ_{global} [37].

III. EXPERIMENTAL SETUP

Experiments were performed with the same polypropylene tetrahedra as in reference [37]. The particles, figure 1a shows an example, were made by mould casting, their edge length is 7 mm and their coefficient of static friction equals 0.8 [60].

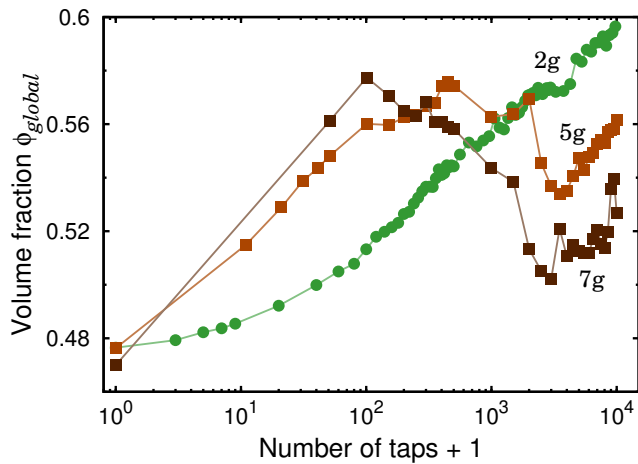


FIG. 2. Compaction of tetrahedra packings for three different tapping strengths $\Gamma = 2g, 5g$ and $7g$.

A. Preparing packings

Packings were prepared by tapping, starting from a loose initial configuration which was prepared by first filling the particles into a smaller inner cylinder (without bottom) and then releasing them into a larger cylindrical container of diameter 10.4 cm by slowly moving the inner cylinder upwards. Tapping is done with an electromagnetic shaker (LDS model V555) which is driven by a series of individual sinusoidal pulses with a periodic time of 1/3s. The separation between individual pulses is 0.5s, the amplitude of the sinusoidal motion is chosen such that the peak acceleration Γ corresponds to either 2g, 5 g, or 7g where g is the acceleration due to gravity.

To monitor the evolution of ϕ_{global} during tapping, height profiles of the packing are measured in regular intervals with a laser distance sensor (MicroEpsilon ILD1402) mounted on a horizontal translation stage. These readings are then corrected for boundary effects by calibrating them with the bulk ϕ_{global} values measured from the tomographic reconstructions.

Figure 2 demonstrates the evolution of ϕ_{global} with the number of taps. For a tapping strength $\Gamma = 2g$ there is a monotonic increase in ϕ_{global} . In contrast, at $\Gamma = 5g$ and $7g$ the volume fraction first increases, then decreases and finally increases again. In none of the experiments a steady state is reached; in reference [37] it is shown that at least 10^5 taps are needed at $\Gamma = 2g$ for reaching a plateau in ϕ_{global} .

B. Image analysis

After the packings have been prepared, three-dimensional images of the geometrical arrangement of particles are obtained by X-ray tomography (Nanotom, GE) with a resolution of 100 μm per voxel. Particles are

then identified by a two step algorithm [37] involving a cross-correlation with an inscribed sphere and a steepest ascend gradient search; the particle detection rates are better than 99.8 %. After the positions and orientations of all particles are known, the number and type of contacts is computed for each particle.

As shown in the supplements of reference [37] the detection of the total number of contacts has an approximate statistical error of ± 0.2 . Unfortunately, we can not derive an error estimate for the algorithm assigning the different contact types. We will therefore consider $\pm 0.2 m_i$ as a best case approximation of our actual errors; this corresponds to ± 0.3 for C_{point} , ± 0.5 for C_{EF} , and ± 0.6 for C_{FF} .

Figure 1c displays a rendering of a cross section through the bulk of a sample where the individual tetrahedra are color coded according to their number of constraints. For the further analysis only particles with a center of mass to container wall distance of at least 2 particle side lengths are retained. This corresponds to 2457 to 3893 tetrahedra per packing as shown in table I.

The Set-Voronoi cells of the tetrahedra were computed using the program `Pome1o` [15] which first discretizes the surface of each particle by spawning points on it, then performs a standard Voronoi tessellation based on all surface points, and finally merges all the standard Voronoi cells on the surface of a given particle to obtain its Set-Voronoi cell. In this work, we resolve each tetrahedra with 514 surface points; figure 1b gives an example of the resolution of such a Set-Voronoi cell. In order to account for the imperfections of both our particles and the image processing, we modify the position of the surface points in two ways: a) we replace the four sharp vertices of the tetrahedra with rounded caps. These cap are approximated by spheres with a radius of $\approx 5\%$ of the side length of a tetrahedron. And b) we shrink the apparent particle size by 1 % in order to avoid artifacts due to overlaps. ϕ_{local} of the individual particles is then computed by dividing the tetrahedra volume by the volume of the Set-Voronoi cells.

The shape of the Set-Voronoi cells is analyzed with the help of Minkowski Tensors of rank two, computed with the program `Karambola` [61]. More specifically we compute for each Set-Voronoi cell the Minkowski Tensor $W_0^{2,0}$ which bears a resemblance to the moment of inertia tensor of the cell. The isotropy index $\beta_0^{2,0}$ is then the eigenvalue ratio of the smallest to the largest eigenvalue of $W_0^{2,0}$. Thus for a perfectly isotropic cell, $\beta_0^{2,0}$ will equal one; with increasing anisotropy the value will decrease. Averaging over all particles in the core of the sample we obtain a global isotropy index $\langle \beta_0^{2,0} \rangle$, for which the origin is the centroid of the Set-Voronoi cell.

TABLE I. Volume fraction ϕ_{global} , Standard deviation of the local volume fraction distribution σ , total constraint number C , contribution of the three different contact types (F2F, E2F, point), Voronoi cell isotropy index $\langle \beta_0^{2,0} \rangle$, and number N of tetrahedra analyzed.

name	symbol	ϕ_{global}	σ	C	C_{F2F}	C_{E2F}	C_{point}	$\langle \beta_0^{2,0} \rangle$	N
10G2	○	0.482	0.051	14.4	0.81	5.8	7.7	0.678	3421
20G2	●	0.481	0.048	13.1	0.39	5.2	7.5	0.690	3425
400G2	□	0.531	0.048	15.5	0.63	6.3	8.5	0.724	3778
10000G7	■	0.526	0.060	13.7	0.80	5.6	7.4	0.708	2457
1600G2	△	0.545	0.052	16.0	1.05	6.6	8.4	0.728	3893
10000G5	▲	0.551	0.059	15.0	1.09	6.1	7.8	0.718	2580

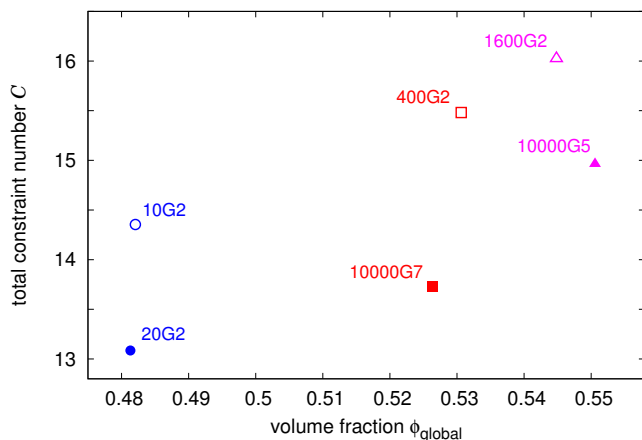


FIG. 3. History dependent preparation. By choosing the number and strength of taps during preparation, we prepare three pairs of packings with approximately the same ϕ_{global} but different values of C .

IV. RESULTS

A. History dependence of the average constraint number

As already shown in [37], the average number of constraints in a tetrahedra packing does not only depend on ϕ_{global} but also on the tapping protocol used to prepare the sample. This history dependence allows us to prepare three pairs of packings with each approximately identical ϕ_{global} but different values in C . These pairs are indicated by open and closed symbols in figure 3. The naming scheme we will use in the following is based on nGa where n stands of the number of taps applied and a corresponds to the acceleration of these taps. I.e. packing 1600G2 has been tapped 1600 times at 2 g.

The two denser pairs of packings are formed by a more constraint packing prepared by tapping the sample with 2 g and a less constraint packing that has been tapped with 5 g and 7 g. Their names are 400G2 - 10000G7 and 1600G2 - 10000G5. The third pair represents fluctuation of the initial preparation by comparing two different ex-

perimental runs both tapped at 2g: 10G2 - 20G2. All four of the samples tapped at 2 g were also included in reference [37]; the particle positions of all six experiments discussed in this paper can be downloaded from Zenodo [62].

Table I displays the ϕ_{global} and C values of all six experiments discussed in this paper. Moreover, the table also shows the contributions of the three different contact types, C_{F2F} , C_{E2F} , and C_{point} , towards the total number of constraints. In all experiments the point contacts contribute with 52 to 57 % the majority to the total constraint number while the face-to-face contacts provide only 3 to 7 % of C ; even though their constraint multiplier m is twice as large as m of the point contacts. We will provide a more detailed analysis of the contribution of the different contact types in section IV B 2.

Table I shows also that the average isotropy index $\langle \beta_0^{2,0} \rangle$ is history-dependent: for the two marginally tapped samples the lower constraint packing is composed of more isotropic Voronoi cells. For the two pairs tapped at different g values, the more constraint packings are more isotropic. This behavior is in contrast to sphere packings where it was shown in [36] that $\langle \beta_0^{2,0} \rangle$ is independent of the preparation; only increasing monotonously with ϕ_{global} . In section IV B 3 we present a local analysis of $\langle \beta_0^{2,0} \rangle$.

B. A local view on tetrahedra packings

As already discussed in the introduction, a global model, i.e. understanding C as a function of ϕ_{global} , is only appropriate for compressible particles where pressure acts as a hidden variable controlling both C and ϕ_{global} [29]. Hard and frictional particles possess no mechanism how ϕ_{global} could control the number of contacts they form. And even if we assume the existence of a particle scale demon, this demon would be unable to compute ϕ_{global} by averaging the ϕ_{local} values of the surrounding particles because these values are spatially correlated [63, 64].

Because the formation of contacts in granular materials is a local process, we need to describe it with locally defined variables. The most important of these is ϕ_{local} :

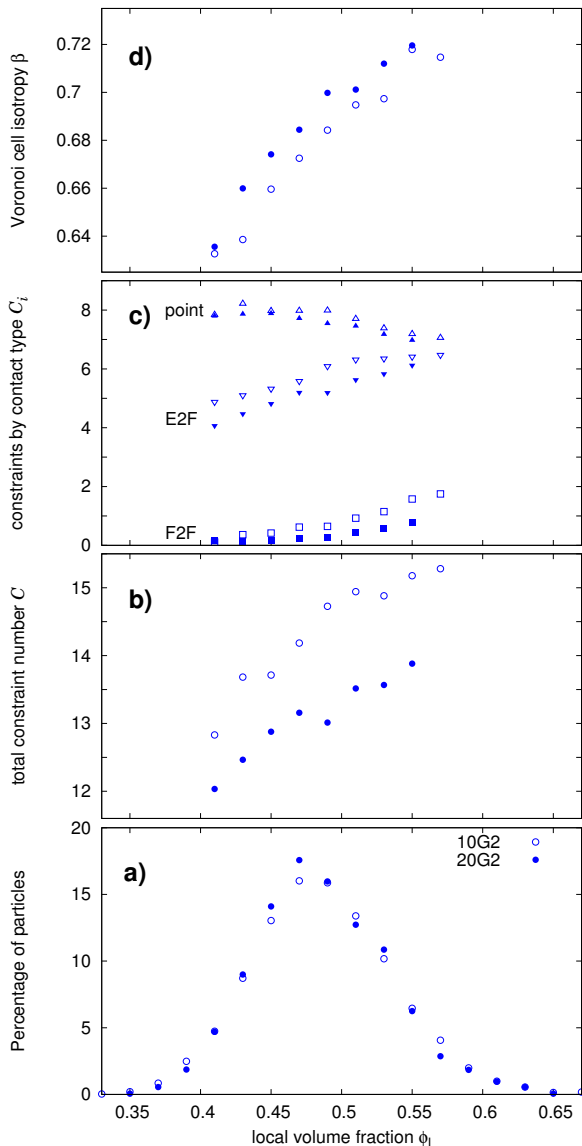


FIG. 4. Comparing two packings which have been only weakly excited (10 respectively 20 taps at 2g) after filling of the container. Their distribution of local volume fractions (a) is identical within experimental errors. The total number of constraints (b) is consistently higher for experiment 10G2, this increase is due to all three contact types as shown in panel c). Contrary to the E2F and F2F contacts, the slope $dC_{point}/d\phi_{local}$ is negative. Finally the Voronoi cell isotropy (d) is larger for the particles which are less constraint. Data points in panels b to d correspond to all bins which contain more than 3 % of the totally number of particles.

it has been shown experimentally [19, 65] that in packings of spheres the most likely contact number of a particles depends only on ϕ_{local} . And *not* on ϕ_{global} . In a first approximation, this locality of the contact formation also holds true for ellipsoids packings where next to ϕ_{local} only the aspect ratio α of the particles is required to know for

predicting the average contact number [19].

For the highly anisotropic tetrahedra, it can be expected that both the shape of the free volume surrounding them, and their relative orientation with respect to the neighboring particles might influence the number of contacts they form. We will describe the former with the isotropy index $\beta_0^{2,0}$ of the Voronoi cells and the latter by the contribution of the individual contact types C_i (where we acknowledge that the latter choice blurs the line between control parameter and result).

The results of our local analysis can be found in figure 4 for the two only marginally shaken packings and in figure 5 for the comparison of the different tapping strengths 2 g and 5/7 g.

1. Distribution of local volume fractions

The harmonic mean of ϕ_{local} (which is how ϕ_{global} is defined for packings of monodisperse particles) is roughly the same within each pair of tetrahedra packings. For spheres [19] one could therefore expect that their C values are also identical. A possible explanation for their in fact different values of C would be the following idea: As in the case of spheres and ellipsoids, there exist some universal, nonlinear functions for $C_i(\phi_{local})$. But at the same time the distributions of the ϕ_{local} values of the two samples are skewed in different directions, resulting in different mean values of C .

However, Figures 4a, 5a, and 5b show that this idea does not apply: There is a small shift corresponding to the slightly different mean values and a small change in the width of the distribution (quantified below), but no pronounced asymmetry.

For spheres and ellipsoids it has been shown [19] that the standard deviation σ of the distribution of the ϕ_{local} values does only depend on the harmonic mean of ϕ_{local} , not even the aspect ratio of the ellipsoids. In table I the σ of our experiments are listed. The σ value of 10G2 is 6.5% larger than the one of its less constraint partner; which seems to be within experimental errors. When comparing the pairs of packings created with different accelerations, the less constraint packings have the broader distributions; the σ value of 10000G7 is 25%, the σ of 10000G5 is 14 % larger than their counterparts. We note however, that such a global analysis is susceptible to spatial gradients within the sample. While for all other samples the fluctuations of ϕ_{local} as a function of height are smaller than ± 0.01 , ϕ_{local} of 10000G7 changes ≈ 0.03 . This explains to some extent the larger σ . In summary, the differences in σ seem to be rather small between the samples.

2. Contact probabilities depend on local volume fraction

A more detailed analysis on how C depends on ϕ_{local} is shown in figures 4b, 5c, and 5d. In all three pairs

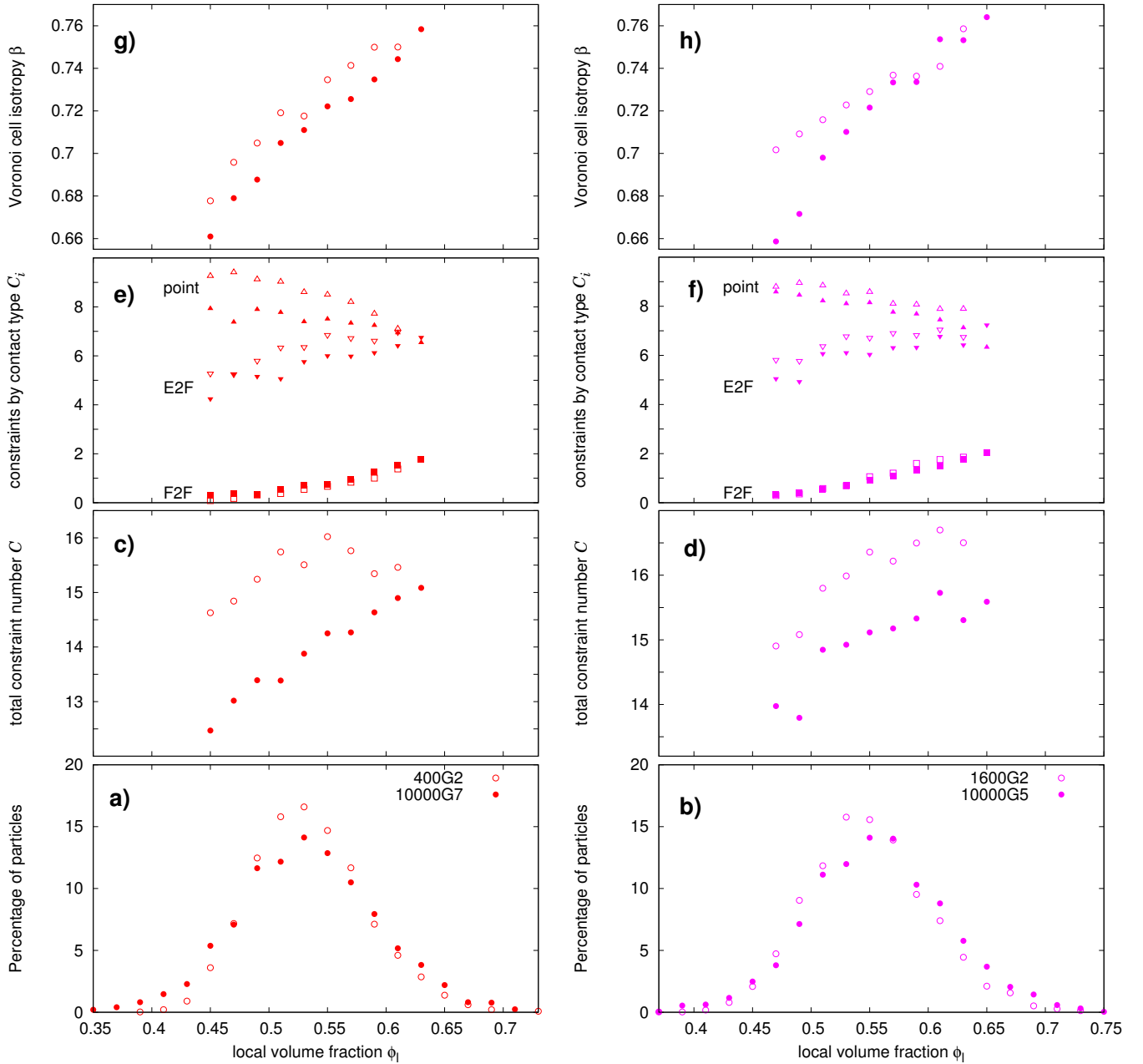


FIG. 5. Comparing pairs of packings which have been tapped at 2g (open symbols) respectively 5g and 7g (closed symbols). For both pairs the distribution of local volume fractions (a) of the higher constraint packing is narrower. Panels e) and f) show that the increase in total C (displayed in panels c) and d)) originates only from the E2F and point contacts. Similar to figure 4c the slope C_{point} with respect to ϕ_{local} is negative. However, in contrast to figure 4d, the Voronoi cell isotropy (shown in panels g) and h) is larger for the more constraint particles. Data points in panels c) to h) correspond to all bins which contain more than 3 % of the totally number of particles.

of experiments the values of $C(\phi_{local})$ are consistently larger for the higher constraint packing. However, the functional form of the $C(\phi_{local})$ curves is not identical. $C(\phi_{local})$ increases monotonically for both marginally tapped samples in figure 4b; the two curves are only shifted vertically against each other. The situation is

more complex for the two pairs tapped with different strengths (figure 5c) and d): for the packings 400G2 $C(\phi_{local})$ seems to approach a plateau, for the other three packings $C(\phi_{local})$ increases monotonically but with different slopes.

As described in section II, the total number of con-

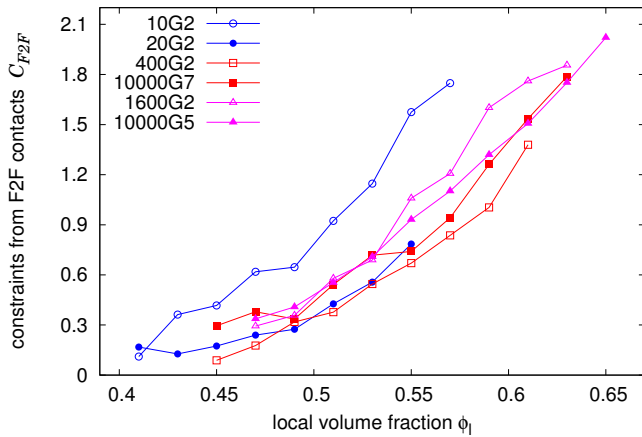


FIG. 6. Constraints due to F2F contacts seem to fall on a universal curve for samples which have been sufficiently tapped (i.e. all samples except for 10G2). Included are all bins in ϕ_{local} which amount to at least 3 % of the total number of particles.

straints C equals $\sum_i C_i$ where i goes over the three contact types. Figures 4c, 5e, and 5f display how the contribution of the three different contact types changes with ϕ_{local} . As already indicated by table I, point contacts provide the largest contribution to C , this is also true for all individual values of ϕ_{local} . Interestingly however, the slope $dC_{\text{point}}/d\phi_{\text{local}}$ is negative while it is positive for the E2F and F2F contacts, as it is for contacts between spheres or ellipsoids [19]. This agrees with the intuitive notion that the closer two tetrahedra get to each other, the more likely it is that their flat faces or straight edges align with each other and the corresponding contact changes from a point contact to a higher constrained one.

For all pairs of packings the difference in preparation is visible in the E2F and point contacts: in a first approximation the $C_{E2F}(\phi_{\text{local}})$ and $C_{\text{point}}(\phi_{\text{local}})$ curves are shifted vertically while their average slope is preserved.

The situation is different for the F2F contacts: for the pairs tapped at different accelerations the $C_{F2F}(\phi_{\text{local}})$ curves fall on top of each other. Figure 6 demonstrates that this agreement goes even further: with the exception of the loose 10G2 sample all other $C_{F2F}(\phi_{\text{local}})$ curves coincide within experimental errors. Which points to the existence of a preparation-independent master function controlling the number of F2F contacts in samples which have been sufficiently tapped.

Some motivation for this different behavior of the F2F contacts can be derived from the high value of their constraint multiplier m_{F2F} : Once a particle has formed an F2F contact with another particle, all three rotational degrees of freedom are completely blocked for both particles. Any additional F2F contact (i.e. increase in C_{F2F}) depends therefore solely on the capability of another incoming particle to align itself such that there is a 180

degree angle between the face normal vectors. The probability that such a rotation is possible will depend strongly on the available space (i.e. ϕ_{local}).

In contrast, pairs of particles which have established an E2F or point contact between themselves, retain one or even three rotational degrees of freedom to facilitate another contact. Which means that geometrical factors, other than ϕ_{local} , will play a role in determining the probability if another contact of the same type can be formed.

3. Voronoi cell isotropy

Figures 4d, 5g, and 5h display the monotonic increase of the isotropy index $\beta_0^{2,0}$ with ϕ_{local} in all our experiments. While such an increase is in agreement with the results for sphere packings [36], the fact that there is no universal curve for $\beta_0^{2,0}(\phi_{\text{local}})$ differs from the behavior of spheres but is compatible with packings of ellipsoids [66].

Moreover, the $\beta_0^{2,0}(\phi_{\text{local}})$ curves reinforce the result already shown in table I: for the only marginally tapped samples the lower constraint packing contains the more isotropic Voronoi cells, for the samples tapped at different levels of g, the higher constraint packings are more isotropic. This signifies that $\beta_0^{2,0}$ is *not* likely to be the hidden parameter connecting the preparation history with the constraint number of the packing.

C. Influence of electrostatics?

A possible candidate for the physical parameter controlling the differences between the packings shaken at different accelerations are electrostatic interactions between the particles. It has recently been shown [67] that electric charges change the contact probabilities in bidisperse sphere packings. For tetrahedra we did observe that in the experiments at 5g and 7g more (polypropylene) tetrahedra did stick to the (PMMA) sidewalls of the shaking container than in the experiments at 2g. And because mixing will distribute charges inside the sample, they would also qualify as a locally defined parameter. However, we could expect that such charges would influence the formation of F2F contacts most (due to their extended proximity between the surfaces). In contrast to this argument, figure 6 shows that the F2F contacts are the least involved in the differences between the packings.

V. CONCLUSIONS

Because tetrahedra have four flat faces, their packings do not only possess point contacts similar to sphere packings but also edge-to-face and face-to-face contacts which fix larger numbers of geometrical constraints than point contacts. The number of point and edge-to-face contacts a given tetrahedron forms can not be predicted from the

global or local volume fraction; the preparation history seems to be encoded in still another parameter. In contrast, the formation of face-to-face contacts in sufficiently tapped samples seems to be a function of the local volume fraction alone, increasing with increasing proximity between particles.

While the isotropy of the Voronoi volume shape, and to some extent also the width of the local volume fraction distribution, do depend on the preparation history of the packing, neither of these two parameters qualifies as the missing control parameter. Our results constitute therefore solely a phenomenological description of the history-

dependence in tetrahedra packings. While they neither support nor rule out the feasibility of a mean-field approach, they imply that the jamming paradigm in its present form will not be an adequate description of the contact formation. More work is needed.

ACKNOWLEDGMENTS

We acknowledge experimental support by Wolf Keiderling.

-
- [1] Farhang Radjaï and Stéphane Roux, “The physics of granular media,” (Wiley-VCH, Weinheim, 2004) pp. 165–187.
 - [2] Luis A. Pugnaloni, Iván Sánchez, Paula A. Gago, Jos Damas, Iker Zuriguel, and Diego Maza, “Towards a relevant set of state variables to describe static granular packings,” *Physical Review E* **82**, 050301 (2010).
 - [3] Luis Ariel Pugnaloni, José Damas, Iker Zuriguel, and Diego Maza, “Master curves for the stress tensor invariants in stationary states of static granular beds. Implications for the thermodynamic phase space,” *Papers in Physics* **3**, 030004 (2011).
 - [4] S. Ardanza-Trevijano, Iker Zuriguel, Roberto Arévalo, and Diego Maza, “Topological analysis of tapped granular media using persistent homology,” *Physical Review E* **89**, 052212 (2014).
 - [5] L. Vanel and E. Clément, “Pressure screening and fluctuations at the bottom of a granular column,” *Euro. Phys. J. B* **11**, 525–533 (1999).
 - [6] J.F. Wambaugh, R.R. Hartley, and R.P. Behringer, “Force networks and elasticity in granular silos,” *Euro. Phys. J. E* **32**, 135–145 (2010).
 - [7] Randy Back, “Frictional effects on mass measurements in a column of glass beads,” *Gran. Mat.* **13**, 723–729 (2011).
 - [8] Christophe Perge, María Alejandra Aguirre, Paula Alejandra Gago, Luis A. Pugnaloni, Denis Le Tourneau, and Jean-Christophe Géminard, “Evolution of pressure profiles during the discharge of a silo,” *Phys. Rev. E* **85**, 021303 (2012).
 - [9] Loic Vanel, Daniel Howell, D. Clark, R. P. Behringer, and Eric Clément, “Memories in sand: Experimental tests of construction history on stress distributions under sandpiles,” *Phys. Rev. E* **60**, R5040 (1999).
 - [10] Christophe Josserand, Alexei V. Tkachenko, Daniel M. Mueth, and Heinrich M. Jaeger, “Memory effects in granular materials,” *Phys. Rev. Lett.* **85**, 3632–3635 (2000).
 - [11] M. Nicolas, P. Duru, and O. Pouliquen, “Compaction of a granular material under cyclic shear,” *Euro. Phys. J. E* **3**, 309–314 (2000).
 - [12] A. Prados and E. Trizac, “Kovacs-like memory effect in driven granular gases,” *Phys. Rev. Lett.* **112**, 198001 (2014).
 - [13] N.N. Medvedev, “Application of the Voronoi-Delone method to description of structure of intersphere space in polydisperse systems,” *Doklady Physical Chemistry* **337** (1994).
 - [14] Fabian M. Schaller, Sebastian C. Kapfer, Myfanwy E. Evans, Matthias J.F. Hoffmann, Tomaso Aste, Mohammad Saadatfar, Klaus Mecke, Gary W. Delaney, and Gerd E. Schröder-Turk, “Set voronoi diagrams of 3d assemblies of aspherical particles,” *Philosophical Magazine* **93**, 3993 – 4017 (2013).
 - [15] Simon Weis, Philipp W. A. Schönhöfer, Fabian M. Schaller, Matthias Schröter, and Gerd E. Schröder-Turk, “Pomelo, a tool for computing Generic Set Voronoi Diagrams of Aspherical Particles of Arbitrary Shape,” *EPJ Web of Conferences* **140**, 06007 (2017).
 - [16] Andrea J. Liu and Sidney R. Nagel, “The jamming transition and the marginally jammed solid,” *Ann. Rev. Cond. Matt. Phys.* **1**, 347–369 (2010).
 - [17] Martin van Hecke, “Jamming of soft particles: geometry, mechanics, scaling and isostaticity,” *J. Phys.: Condens. Matter* **22**, 033101 (2010).
 - [18] The limited choices of experimental preparation protocols might have influenced this results: it has been shown numerically by Agnolin and Roux (*Phys. Rev. E* **76**, 061302, 2007) that even for spheres the value of Z can differ for identical ϕ_{global} .
 - [19] Fabian M. Schaller, Max Neudecker, Mohammad Saadatfar, Gary W. Delaney, Gerd E. Schröder-Turk, and Matthias Schröter, “Local Origin of Global Contact Numbers in Frictional Ellipsoid Packings,” *Physical Review Letters* **114**, 158001 (2015).
 - [20] Chaoming Song, Ping Wang, and Hernán A. Makse, “A phase diagram for jammed matter,” *Nature* **453**, 629–632 (2008).
 - [21] Adrian Baule, Romain Mari, Lin Bo, Louis Portal, and Hernn A. Makse, “Mean-field theory of random close packings of axisymmetric particles,” *Nat Commun* **4**, 1–11 (2013).
 - [22] Adrian Baule and Hernán A. Makse, “Fundamental challenges in packing problems: from spherical to non-spherical particles,” *Soft Matter* **10**, 4423–4429 (2014).
 - [23] Nishant Kumar and Stefan Luding, “Memory of jammingmultiscale models for soft and granular matter,” *Granular Matter* **18**, 58 (2016).
 - [24] Stefan Luding, “So much for the jamming point,” *Nature Phys.* **12**, 531–532 (2016).
 - [25] Leonardo E. Silbert, Deniz Ertas, Gary S. Grest, Thomas C. Halsey, and Dov Levine, “Geometry of frictionless and frictional sphere packings,” *Phys. Rev. E* **65**,

- 031304 (2002).
- [26] H. P. Zhang and H. A. Makse, “Jamming transition in emulsions and granular materials,” *Phys. Rev. E* **72**, 011301 (2005).
- [27] Kostya Shundyak, Martin van Hecke, and Wim van Saarloos, “Force mobilization and generalized isostaticity in jammed packings of frictional grains,” *Phys. Rev. E* **75**, 010301 (2007).
- [28] S. Henkes, M. van Hecke, and W. van Saarloos, “Critical jamming of frictional grains in the generalized isostaticity picture,” *Europhys. Lett.* **90**, 14003 (2010).
- [29] Matthias Schröter, “A local view on the role of friction and shape,” *EPJ Web of Conferences* **140**, 01008 (2017).
- [30] Brian P. Tighe, Jacco H. Snoeijer, Thijs J. H. Vlugt, and Martin van Hecke, “The force network ensemble for granular packings,” *Soft Matter* **6**, 2908–2917 (2010).
- [31] Olivier Tsoungui, Denis Vallet, and Jean-Claude Charmet, “Use of contact area trace to study the force distributions inside 2d granular systems,” *Granular Matter* **1**, 65–69 (1998).
- [32] Joshua A. Dijksman, Nicolas Brodu, and Robert P. Behringer, “Refractive index matched scanning and detection of soft particles,” *Review of Scientific Instruments* **88**, 051807 (2017).
- [33] Karen E. Daniels, Jonathan E. Kollmer, and James G. Puckett, “Photoelastic force measurements in granular materials,” *Review of Scientific Instruments* **88**, 051808 (2017).
- [34] T. S. Majmudar and R. P. Behringer, “Contact force measurements and stress-induced anisotropy in granular materials,” *Nature* **435**, 1079–1082 (2005).
- [35] T. Aste, T. Di Matteo, M. Saadatfar, T. J. Senden, Matthias Schröter, and Harry L. Swinney, “An invariant distribution in static granular media,” *Europhys. Lett.* **79**, 24003 (2007).
- [36] G. E. Schröder-Turk, W. Mickel, M. Schröter, G. W. Delaney, M. Saadatfar, T. J. Senden, K. Mecke, and T. Aste, “Disordered spherical bead packs are anisotropic,” *Europhys. Lett.* **90**, 34001 (2010).
- [37] Max Neudecker, Stephan Ulrich, Stephan Herminghaus, and Matthias Schröter, “Jammed frictional tetrahedra are hyperstatic,” *Phys. Rev. Lett.* **111**, 028001 (2013).
- [38] Bo Zhao, Xizhong An, Yang Wang, Quan Qian, Xiaohong Yang, and Xudong Sun, “DEM dynamic simulation of tetrahedral particle packing under 3d mechanical vibration,” *Powder Technology* **317**, 171–180 (2017).
- [39] Alexander Jaoshvili, Andria Esakia, Massimo Porrati, and Paul M. Chaikin, “Experiments on the random packing of tetrahedral dice,” *Phys. Rev. Lett.* **104**, 185501 (2010).
- [40] Amir Haji-Akbari, Michael Engel, Aaron S. Keys, Xiaoyu Zheng, Rolfe G. Petschek, Peter Palffy-Muhoray, and Sharon C. Glotzer, “Disordered, quasicrystalline and crystalline phases of densely packed tetrahedra,” *Nature* **462**, 773–777 (2009).
- [41] Yang Jiao and Salvatore Torquato, “Maximally random jammed packings of Platonic solids: Hyperuniform long-range correlations and isostaticity,” *Physical Review E* **84**, 041309 (2011).
- [42] Yoav Kallus and Veit Elser, “Dense-packing crystal structures of physical tetrahedra,” *Physical Review E* **83**, 036703 (2011).
- [43] Jian Zhao, Shuixiang Li, Weiwei Jin, and Xuan Zhou, “Shape effects on the random-packing density of tetrahedral particles,” *Physical Review E* **86**, 031307 (2012).
- [44] Pablo F. Damasceno, Michael Engel, and Sharon C. Glotzer, “Crystalline Assemblies and Densest Packings of a Family of Truncated Tetrahedra and the Role of Directional Entropic Forces,” *ACS Nano* **6**, 609–614 (2012).
- [45] Weiwei Jin, Peng Lu, and Shuixiang Li, “Evolution of the dense packings of spherotetrahedral particles: from ideal tetrahedra to spheres,” *Scientific Reports* **5**, srep15640 (2015).
- [46] Kyle C. Smith, Meheboob Alam, and Timothy S. Fisher, “Athermal jamming of soft frictionless platonic solids,” *Phys. Rev. E* **82**, 051304 (2010).
- [47] Kyle C. Smith, Timothy S. Fisher, and Meheboob Alam, “Isostaticity of constraints in amorphous jammed systems of soft frictionless platonic solids,” *Phys. Rev. E* **84**, 030301 (2011).
- [48] Kyle C. Smith, Ishan Srivastava, Timothy S. Fisher, and Meheboob Alam, “Variable-cell method for stress-controlled jamming of athermal, frictionless grains,” *Phys. Rev. E* **89**, 042203 (2014).
- [49] A. T. Cadotte, J. Dshemuchadse, P. F. Damasceno, R. S. Newman, and S. C. Glotzer, “Self-assembly of a space-tessellating structure in the binary system of hard tetrahedra and octahedra,” *Soft Matter* **12**, 7073–7078 (2016).
- [50] Shuixiang Li, Peng Lu, Weiwei Jin, and Lingyi Meng, “Quasi-random packing of tetrahedra,” *Soft Matter* **9**, 9298–9302 (2013).
- [51] Lufeng Liu, Peng Lu, Lingyi Meng, Weiwei Jin, and Shuixiang Li, “Excluded volumes of clusters in tetrahedral particle packing,” *Physics Letters A* **378**, 835–838 (2014).
- [52] Weiwei Jin, Peng Lu, Lufeng Liu, and Shuixiang Li, “Cluster and constraint analysis in tetrahedron packings,” *Physical Review E* **91**, 042203 (2015).
- [53] S. Torquato and Y. Jiao, “Dense packings of the platonic and archimedean solids,” *Nature* **460**, 876–879 (2009).
- [54] Yoav Kallus, Veit Elser, and Simon Gravel, “Dense periodic packings of tetrahedra with small repeating units,” *Discrete & Computational Geometry* **44**, 245–252 (2010).
- [55] S. Torquato and Y. Jiao, “Exact constructions of a family of dense periodic packings of tetrahedra,” *Phys. Rev. E* **81**, 041310 (2010).
- [56] Elizabeth Chen, Michael Engel, and Sharon Glotzer, “Dense crystalline dimer packings of regular tetrahedra,” *Discrete & Computational Geometry* **44**, 253–280 (2010).
- [57] Jessica Baker and Arshad Kudrolli, “Maximum and minimum stable random packings of platonic solids,” *Phys. Rev. E* **82**, 061304 (2010).
- [58] Athanasios G. Athanassiadis, Marc Z. Miskin, Paul Kaplan, Nicholas Rodenberg, Seung Hwan Lee, Jason Merritt, Eric Brown, John Amend, Hod Lipson, and Heinrich M. Jaeger, “Particle shape effects on the stress response of granular packings,” *Soft Matter* **10**, 48–59 (2013).
- [59] Heinrich M. Jaeger, “Celebrating soft matters 10th anniversary: Toward jamming by design,” *Soft Matter* **11**, 12–27 (2015).
- [60] μ_s is computed from the tangens of the inclination angle where a face to face contact starts to slide.
- [61] G. E. Schröder-Turk, W. Mickel, S. C. Kapfer, F. M. Schaller, B. Breidenbach, D. Hug, and K. Mecke, “Minkowski tensors of anisotropic spatial structure,” *New Journal of Physics* **15**, 083028 (2013).
- [62] DOI from Zenodo; data upload is only possible after pa-

per is accepted by a journal.

- [63] F Lechenault, F da Cruz, O Dauchot, and E Bertin, “Free volume distributions and compactivity measurement in a bidimensional granular packing,” *J. Stat. Mech.* **2006**, P07009 (2006).
- [64] Song-Chuan Zhao, Stacy Sidle, Harry L. Swinney, and M Schröter, “Correlation between voronoi volumes in disc packings,” *Europhys. Lett.* **97**, 34004 (2012).
- [65] T Aste, M Saadatfar, and T J Senden, “Local and global relations between the number of contacts and density in monodisperse sphere packs,” *J. Stat. Mech.: Theory and Exp.* **2006**, P07010 (2006).
- [66] Fabian M. Schaller, Sebastian C. Kapfer, James E. Hilton, Paul W. Cleary, Klaus Mecke, Cristiano De Michele, Tanja Schilling, Mohammad Saadatfar, Matthias Schröter, Gary W. Delaney, and Gerd E. Schröder-Turk, “Non-universal Voronoi cell shapes in amorphous ellipsoid packs,” *EPL (Europhysics Letters)* **111**, 24002 (2015).
- [67] André Schella, Simon Weis, and Matthias Schröter, “Charging changes contact composition in binary sphere packings,” *Physical Review E* **95**, 062903 (2017).